



ELSEVIER

Palaeogeography, Palaeoclimatology, Palaeoecology 193 (2003) 181–200

PALAEO

www.elsevier.com/locate/palaeo

The Dry Holocene Megathermal in Inner Mongolia

Chen-Tung A. Chen^{a,*}, Hsin-Chi Lan^a, Jiann-Yuh Lou^{a,1}, Yan-Cheng Chen^b

^a *Institute of Marine Geology and Chemistry, National Sun Yat-sen University, Kaohsiung 80424, Taiwan*

^b *Institute of Geological Research and Chemical Mines, Ministry of Chemical Industries, Zhuozhou 072754, PR China*

Received 20 March 2002; received in revised form 2 December 2002; accepted 12 December 2002

Abstract

The paleoclimate since 14 kyr BP (¹⁴C age) was reconstructed based on a 16.22-m-long sediment core collected from Lake Yanhaizi, a saline lake located near the northern limit of the East Asian summer monsoon in Inner Mongolia. Coarse sediments were deposited there during a shrinkage phase of the lake when sand dunes reactivated. These sediments have low organic carbon contents but high maturity indices, indicating that they were deposited in an arid environment. By contrast, based on high organic contents and low maturity indices, fine sediments were deposited during periods of high lake stand in a humid environment. It was in general dry between 8.0 and 4.3 kyr BP. The above dry and wet phases are consistent with those recovered from the arid–semiarid transition zone elsewhere, but are unlike the widely perceived humid Holocene Megathermal reported in east China and the newly reconstructed record in the alpine Retreat Lake in Taiwan. The discrepancy may be due to a relative insensitivity to humidity changes in these two areas since they have both been under the total influence of the summer monsoon. On the other hand, much enhanced evaporation over higher monsoon precipitation at Lake Yanhaizi reduces the effective humidity in the warm climate near the northern boundary of the summer monsoon. This also accounts for the fact the high-temperature Holocene Megathermal, as revealed in the Okinawa Trough and the northern South China Sea, is correlated to the dry phases at Lake Yanhaizi. Conversely, the 4–2-kyr BP coldest period in the Holocene corresponds to a wet phase at Lake Yanhaizi.

© 2003 Elsevier Science B.V. All rights reserved.

Keywords: Holocene Megathermal; Inner Mongolia; paleoclimate; East Asian summer monsoon; effective humidity

1. Introduction

The climate of eastern Asia is largely controlled by the East Asian monsoon system which responds to the strength of high-and low-pressure

cells growing and decaying seasonally over the Asian landmass. The monsoon draws winds and moisture mainly from the tropical Philippine and South China seas at its northern boundary of Inner Mongolia during summer, and this results in more precipitation over the northwestern interior of China. The present-day landward limit of summer monsoon precipitation lies in the northeast–southwest direction in Inner Mongolia (Gao, 1962). Consequently, distinct distributions of loess, sandy loess and sand dune landforms

¹ Present address: Department of Marine Science, Chinese Naval Academy, P.O. Box 90175, Tsoying, Kaohsiung, Taiwan.

* Corresponding author. Fax: +886-7-525-5346.

E-mail address: ctchen@mail.nsysu.edu.tw (C.-T.A. Chen).

which reflect the decreasing relative humidity extend from the southeast to the northwest. As a result, the waxing and waning of the summer monsoon intensity control the availability of precipitation in Inner Mongolia and reflect the horizontal migration of the landforms.

During the early to mid-Holocene, the conditions that prevailed were, for the most part, wetter than those today over monsoonal areas, such as those in the Sahara, the Arabian Peninsula, India and eastern Asia (Ritchie and Haynes, 1987; Kutzbach et al., 1996; Enzel et al., 1999). This was in response to increased summer insolation (Kutzbach and Otto-Bliesner, 1982; Kutzbach and Street-Perrott, 1985; COHMAP Members, 1988). A wealth of records from the Chinese Loess Plateau has depicted this past scenario of the East Asian summer monsoon-influenced areas as warm and humid during high-temperature interglacials when the summer monsoon strengthened (Kukla et al., 1988; An et al., 1990); records have also demonstrated that the most humid period of the Holocene was during the warmest Holocene Megathermal in eastern China (Shi et al., 1993). On the other hand, during the last glaciation, global cooling enhanced the Mongolian High-Pressure Zone. At that time, the winter monsoon was greatly strengthened and the summer monsoon significantly weakened (An et al., 1990). However, these records mainly came from the intensively studied Loess Plateau.

Although research on the Mu Us Desert, to the north of the loess, has been carried out in recent years, most of this has been limited to the southern margin of the desert and has poor temporal resolution during the Holocene (Sun et al., 1998a,b, 1999; Sun, 2000; Li et al., 2000). The principal objective of this project is to document and understand decade- to century-scale paleoclimatic variations using detailed sedimentary records from saline lakes in the deserts of Inner Mongolia. This obviously takes advantage of the fact that closed-basin lakes in the deserts are sensitive to the balance between precipitation and evaporation, which is directly linked to atmospheric circulation (Street-Perrott and Roberts, 1983). Analysis of the lacustrine records in the deserts could address how temporal and regional

variations with respect to the monsoon respond to longer-term shifts in the monsoonal paleoclimate, thereby providing high-resolution records that cover a sufficiently long time scale and fully capture the natural range of variability in the monsoonal system. Additionally, it will offer information that is essential for understanding near-term future climatic variations in the monsoonal region. The sediments in the studied lake have indeed preserved a high-resolution record over the last 14 000 yr BP, one of the most complete and detailed sets of Holocene paleoclimatic records obtained within the eastern Asian monsoonal region.

2. Study area

Lake Yanhaizi (108°25'E–108°29'E, 40°06'–40°10'N, 1180 m a.s.l., Fig. 1a) is one of the many hypersaline lakes located 500 km west of Beijing on the Ordos Plateau, Inner Mongolia. It is 800 km from the nearest ocean, the Bohai Sea, and about 1150 km from the East China Sea. The lake covers a maximum area of 18 km², has a maximum water depth of about 0.5 m in summer, and a drainage area of about 2000 km² in the Mu Us Desert (Zhang et al., 1992).

The mean annual temperature is 5.9°C, with a low mean monthly temperature of –12.2°C in January and a high mean monthly temperature of 21.6°C in July. Climatically, the strong seasonal influence of the East Asian monsoon reaches the area during the summer, resulting in rainfall from July to September (Zhang and Lin, 1992). The mean annual precipitation is only 277 mm, concentrated between July and September. However, the mean annual evaporation is 2604 mm, mostly between April and August. The bedrock of the lake is mainly composed of Lower Cretaceous yellow–greenish sandstones belonging to the Dong Sheng and Yijinguolou formations.

3. Materials and methods

Four cores, YA01, YA02, YA03 and YAS03, were drilled in Lake Yanhaizi (Fig. 1b) during

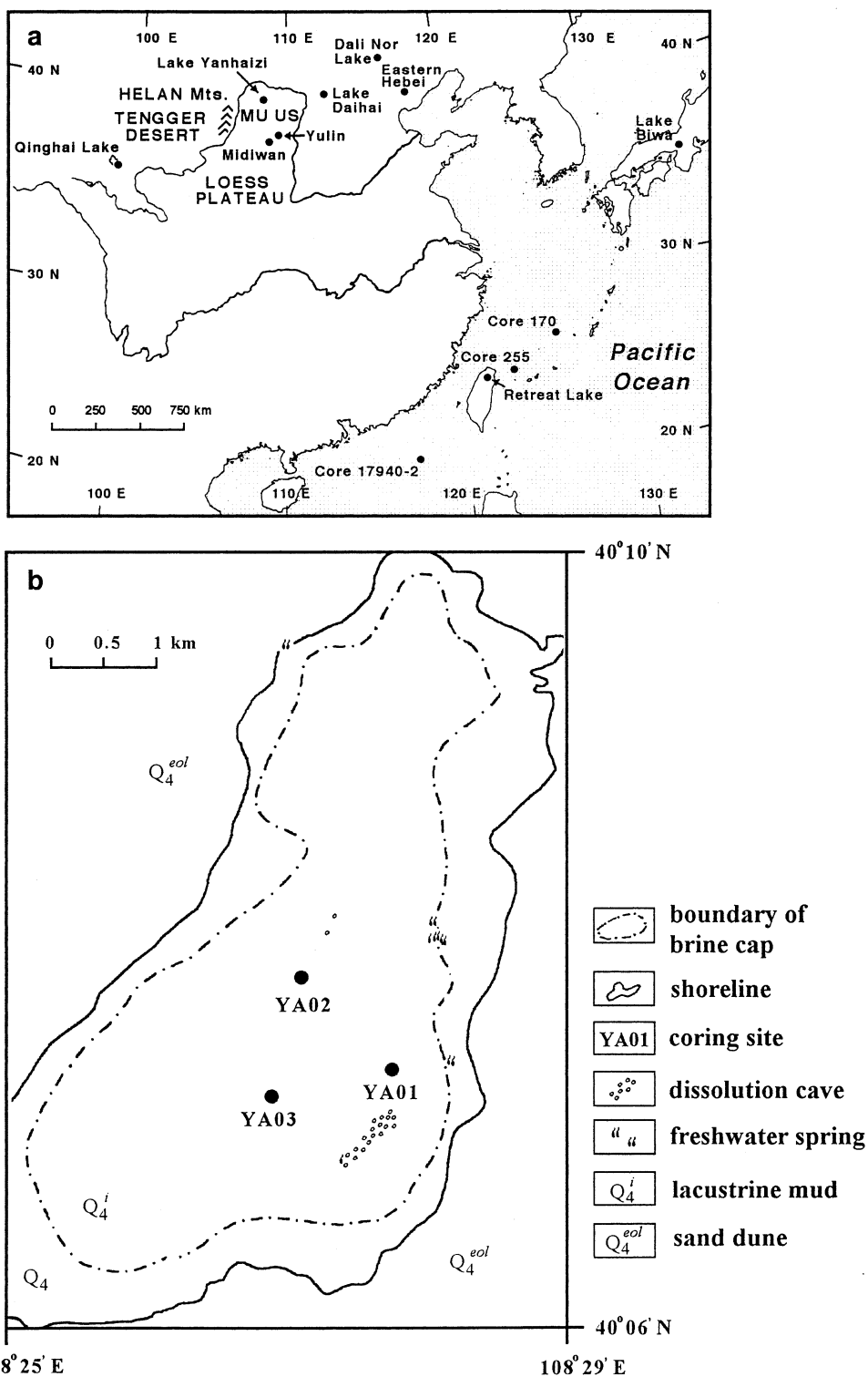


Fig. 1. (a) Map showing the locations of Lake Yanhai and sites of other archives referred to in this paper. (b) Coring sites (YA01, Ya02 and Ya03) in Lake Yanhai.

two consecutive joint drilling programs. The first was executed by the Institute of Geology, Swiss Federal Institute of Technology in Zürich, Switzerland, and the Institute of Geological Research and Chemical Mines, Ministry of Chemical Industries, China, in 1992. The second one was performed in 1997 with all the cores archived in the Institute of Marine Geology and Chemistry, National Sun Yat-sen University (IMGC-NSYSU), Taiwan. The first expedition has been reported by [Bernasconi et al. \(1997\)](#) and covers Lake Hengtongchahannor south of Lake Yanhaizi. For now, most of the analyses have been performed on Core YA01, and these have been supplemented by data from Cores YA02 and YAS03 as well as the lithological variations of Core YA03 and nearby desert sand. Subsampling of the 16.22-m-long Core YA01 was done in the laboratory at 10-cm intervals. The 1-cm-thick samples were then oven-dried at 60°C and utilized in all further studies.

A LECO CHN-932 elemental analyzer was employed to determine carbon content at 950°C. After the samples were repeatedly rinsed with 1 N HCl to remove inorganic carbon, total organic carbon (TOC) was determined by different mixes of NIST (SRM-2704, carbon: 3.348%), LECO-EDTA (carbon: 41.1%, nitrogen: 9.59%) and feldspar powder for calibration ([Lou and Chen, 1997](#)). Precision was $\pm 5\%$ for TOC.

Concentrations of 27 elements (O, Na, Mg, Al, Si, P, S, Cl, K, Ca, Ti, V, Cr, Mn, Fe, Co, Ni, Cu, Zn, Ga, Br, Rb, Sr, Y, Zr, Ba and Pb) were measured with the Rigaku RIX-2000 XRF ([Chen et al., 2001](#)). Five grams of ground powder of each sample was palletized under 20 ton cm^{-12} pressure for 20 min to form a cake with cellulose as backing. Seven standard samples, namely BCSS-1, MESS-1, PACS-1, MAG-1, NIES-2, SRM-2704 and GBW-07314, were used for calibration. Replicate analyses of the same samples gave a precision within 5–10%.

Low-frequency (0.47 kHz) and high-frequency (4.7 kHz) magnetic susceptibility analyses were performed using a Bartington MS-2B sensor which was attached to a MS-2 susceptibility meter. Each sample was measured three times. Minerals were determined with a SIMENS D5000

X-ray powder diffractometer at the Institute of Material Science and Engineering, NSYSU. Conditions were set at 40 kV, 20 mA, and a $\text{CuK}\alpha$ target was chosen with step increases of 0.02°. Grain size analyses were carried out with a Coulter LS-100 laser particle size analyzer (IMGC-NSYSU) following the procedures described by [Janitzky \(1987\)](#): samples gently hand-ground in a quartz pestle and mortar were sieved to remove grains larger than 1000 μm , and then treated with HCl and H_2O_2 to remove carbonate and organic matter. In the final stage, sodium hexametaphosphate was added to prevent clay minerals from flocculating, and the samples received a short period of ultrasonic agitation.

Samples of mostly humin and some organic matter were dated using the AMS at the Rafter Radiocarbon Laboratory, Institute of Geological and Nuclear Sciences, New Zealand, and at the Leibniz-Labor for Radiometric Dating and Isotope Research, Christian-Albrechts-University Kiel, Germany, as well as with the conventional liquid scintillation counting method at the Laboratory of Carbon Dating, Department of Geosciences, National Taiwan University, Taiwan. One concentrated pollen sample was analyzed in the Leibniz-Labor in order to correct for the reservoir effect.

Samples of Core YAS03 were measured for ^{210}Pb with a TENNELEC LB 5100-2800-II counting system in the Radio Isotope Laboratory (IMGC-NSYSU) following the procedure by [Hung and Chung \(1998\)](#). Inorganic stable oxygen and carbon isotope analyses were performed at the Institute of Earth Sciences, Academia Sinica, Taiwan.

4. Results

Core YA01 shows that the upper 3.04 m of the Quaternary sediment is comprised predominantly of mirabilite crystals ($\text{Na}_2\text{SO}_4 \cdot 10\text{H}_2\text{O}$) containing varying amounts of black quartz sand and silt ([Fig. 2a,b](#)). Between 3.04 and 8.29 m, mainly black sand and silty sand are found with the highest abundance between 5.50 and 7.30 m. These become grayish–green between 8.29 and

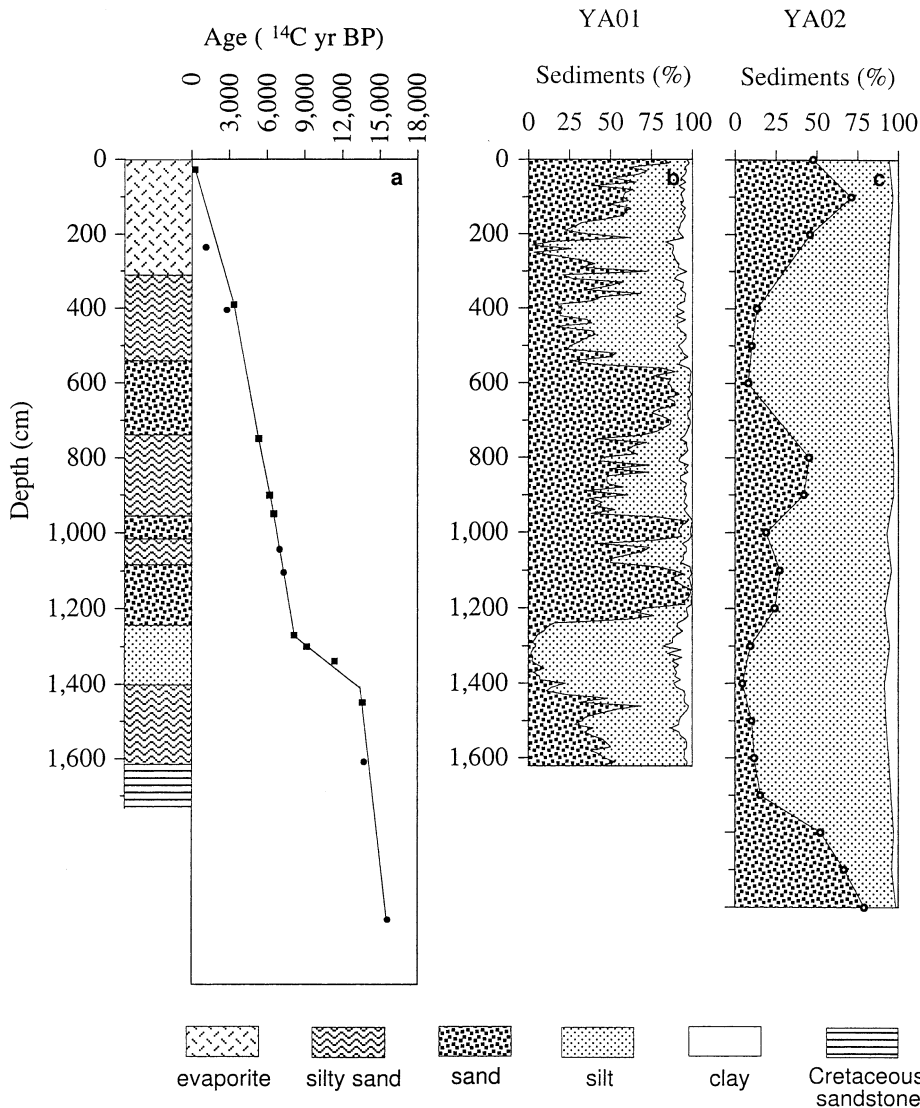


Fig. 2. (a) Radiocarbon chronology of Core YA01. Solid squares (■) stand for ^{14}C dates of YA01, while solid circles (●) denote ^{14}C dates inferred from Core YA02. Different segments of the line represent various age models. (b,c) Variations in lithology with depth for Cores YA01 and YA02, respectively.

11.70 m, where silt and sand are the major components; however, between 9.70 and 12.30 m sand is more abundant. The color becomes black again at 12.70 m, and silt and clay are the major components between 12.30 and 14.20 m. Greyish-green silt and sand are found below 14.20 m, but at 16.22 m sandstone is found. Fossil discrimination on Core YA01 has not yet been performed, but fragments of gastropod of unknown

species are found at depths 12.75, 13.45, 14.74, 17.74, 19.38 and 20.74 m on Core YA02.

^{14}C and calibrated calendar ages using the CALIB 4.3 program (Stuiver et al., 1998) are shown in Table 1; all ages without the extra notation of the calendar year (cal. yr BP or cal. kyr BP) quoted in this paper are in ^{14}C years (yr BP or kyr BP). The chronostratigraphy of the core is plotted in Fig. 2a. Results from the nearby Core

Table 1
Radiocarbon dates for the YA01 sequence

Depth (cm)	Material	$\delta^{13}\text{C}$ (‰)	^{14}C age (^{14}C yr BP)	Calibrated age (cal. yr BP)	Lab. ref. ^a
27	Humin ^b	−24.8	1110 ± 180	1048	NTU2326
390	TOC	−26.4	4213 ± 70	4827	NZA7298
749	Humin	−25.3	6200 ± 340	7157	NTU2228
900	Humin	−24.0	7080 ± 200	7933	NTU2337
950	TOC	−25.7	7398 ± 70	8181	NZA7432
1270	Humin	−24.3	9020 ± 190	10208	NTU2208
1275	Pollen	−25.4	8415 ± 50	9470	KIA7929
1300	Humin	−24.4	10026 ± 44	11549	KIA6431
1339	Humin	−27.8	12263 ± 75	14265	NZA8334
1449	Humin	−30.3	14459 ± 87	17318	NZA8335

^a Lab. reference: NTU, Laboratory of Carbon Dating, Department of Geosciences, National Taiwan University, Taiwan; NZA, Rafter Radiocarbon Laboratory, Institute of Geological and Nuclear Sciences, New Zealand; KIA, Leibniz-Labor for Radiometric Dating and Isotope Research, Christian-Albrechts-University Kiel, Germany.

^b Sample where saline groundwater flows.

YA02 (located more central to the lake; Fig. 1b) at a similar depth and strata (Fig. 2c; Table 2) are also added with no obvious evidence of systematic differences. The deposition rates of the core are more or less constant except for the section between 12.4 and 14.4 m, where the rate is much slower.

In saline lake environments, the reservoir effect is frequently the most important artifact prohibiting accurate carbon dating. Several methods, both indirect and direct, were evaluated to constrain the reservoir effect in Lake Yanhaizi. Extrapolating the ^{14}C ages to the coretop yields an age of 879 yr BP, which is the first indirect indicator of a possible reservoir effect. Further, taking the sedimentation rate, 0.112 cm/yr, calculated from excess ^{210}Pb (Table 3) and assuming that the age of

the coretop is zero and the sedimentation rate is uniform, an age of 195 yr BP is determined for the sample at 0.27 m depth. The ^{14}C age, however, is 1110 ± 180 yr BP (Table 1), making the age difference of 915 yr the second approximation of the reservoir effect.

Next, direct ^{14}C dating of the lake water yields 887 ± 121 yr BP (Table 2) which agrees with the above two values. Finally, because sporopollen is not influenced by the reservoir effect (Regnell, 1992; Zhou et al., 1997), the age of direct dating of the sporopollen concentrated in the sediments provides the fourth approximation. The age of the sporopollen at 12.75 m is 8415 ± 50 yr BP (Table 1). On the other hand, the age of the bulk sample at depth 12.75 m interpolated from the two adjacent dated samples, depths 12.7 and 13.0 m (of

Table 2
Radiocarbon dates for the YA02 sequence and saline water of the lake

Depth (cm)	Material	$\delta^{13}\text{C}$ (‰)	^{14}C age (^{14}C yr BP)	Calibrated age (cal. yr BP)	Lab. ref. ^a
0	Saline water		887 ± 121	788	ASA
236	TOC		1973 ± 264	1923	ASA
405	TOC		3658 ± 123	3978	ASA
1044.5	TOC		7859 ± 207	8627	ASA
1105	TOC		8189 ± 200	9232	ASA
1608	TOC		14571 ± 344	17447	ASA
2030	Humin	−18.7	16450 ± 460	19609	NTU2357

^a Lab. reference: ASA, Institute of Archaeology, Chinese Academy of Social Sciences, China; NTU, Laboratory of Carbon Dating, Department of Geosciences, National Taiwan University, Taiwan.

Table 3
Activities of excess ^{210}Pb for Core YAS03

Depth (cm)	$^{210}\text{Pb}_{\text{ex}}$ (dpm g $^{-1}$)
1	1.60
3	0.90
5	0.43
7	0.25
9	0.18
12	0.00

age 9020 ± 190 and 10026 ± 44 yr BP, respectively), is 9188 yr BP, which is 773 yr older than the age of the sporopollen. Accordingly, 879 yr was taken as the reservoir effect in this study. This is in reasonable agreement with the hard water effect estimated at about 1000–2000 yr for lakes in Inner Mongolia (Ren, 1998).

After subtracting 879 yr, ages were then linearly interpolated for each sample by assuming a uniform sedimentation rate between each major change in the sedimentation rates accompanied by major lithologic changes. The linear sedimentation rates thus obtained vary significantly within the core with high values of 0.157 cm yr^{-1} between 14.2 and 16.22 m and relatively low values of 0.033 cm yr^{-1} between 12.5 and 14.2 m. The variations in the relative contents of sand, silt and clay with age are shown in Fig. 3a.

The TOC values are generally low, between 0.09% and 1.08%. There are three sections with relatively high TOC, between 3100 and 4200, 5800 and 6400, and 8000 and 13400 yr BP (Fig. 3b). The higher values are considered representative of higher biomass productivity in the drainage (Pedersen and Calvert, 1990; Lou and Chen, 1997; Lou et al., 1997). The productivity in an arid area is, in turn, controlled by the effective precipitation (An et al., 1993). Thus, these three segments represent a more humid environment. Desert sand samples from the nearby Mu Us Desert have a TOC content of 0.17%, similar to the values found in the dry segments of the core.

Higher TOC/TN ratios have also been taken to represent higher productivity on land (Lou and Chen, 1997; Meyers, 1997), but the signals here are mixed (Fig. 3c). The absence of data for the last 2.8 kyr BP has resulted from the nitrogen

analysis which was unreliable due to the perturbation caused by the presence of saline minerals. Although the three humid segments in fact do have slightly higher TOC/TN values than the dry ones, i.e. between 4300 and 5900, and 6400 and 8000 yr BP, the oldest dry segment before 13400 yr BP has the highest TOC/TN. This may reflect a preferential decomposition of organic nitrogen. The nearby desert sand samples have a TOC/TN ratio of about 9, similar to that found in the dry segments in the mid-Holocene.

According to Ding et al. (1999), the sand ($> 63 \mu\text{m}$) content, an indicator of sand desert has never been absent since S1-1 (marine isotope stage 5a) in the Yulin section situated in the transitional zone between the Mu Us Desert and the Loess Plateau downwind of the winter monsoon from our study area (Fig. 1a). As a result, Lake Yanhaizi must have also been receiving desert sand since S1-1. Desert sand samples near Lake Yanhaizi are characterized by a rounded, well-sorted texture and have a modal grain size of about $300 \mu\text{m}$ (Fig. 4a). The sediment samples in the dry segments have a similar texture to that of the dune sand (Fig. 4b), implying that the samples were deposited during sand dune or sand sheet progradation periods; that is, during a shrinkage phase of the lake. In contrast, sediment samples in the wet segments have a distinct size mode of about $10\text{--}30 \mu\text{m}$ although some sand is still present (Fig. 4c). We assume that during periods of high lake stand, the periphery of the lake was pushed outward. It is understood that a larger water body would have trapped more aeolian dust (Fryberger et al., 1983) and provided better preservation of these fine wind-carried dusts in the water. At the same time, a higher groundwater table would have sustained the vegetation, which, in turn, would have prevented the sand dune and sand sheet from entering the lake (Nemoto et al., 1997). High precipitation rates also increase the scavenging of aeolian material by rain (Windom, 1975). All of these mechanisms should have left the lake with finer sediments in the humid segments. This is indeed what has been observed in the case of Lake Yanhaizi.

The maturity index is defined as the ratio of feldspars to the sum of feldspars and quartz

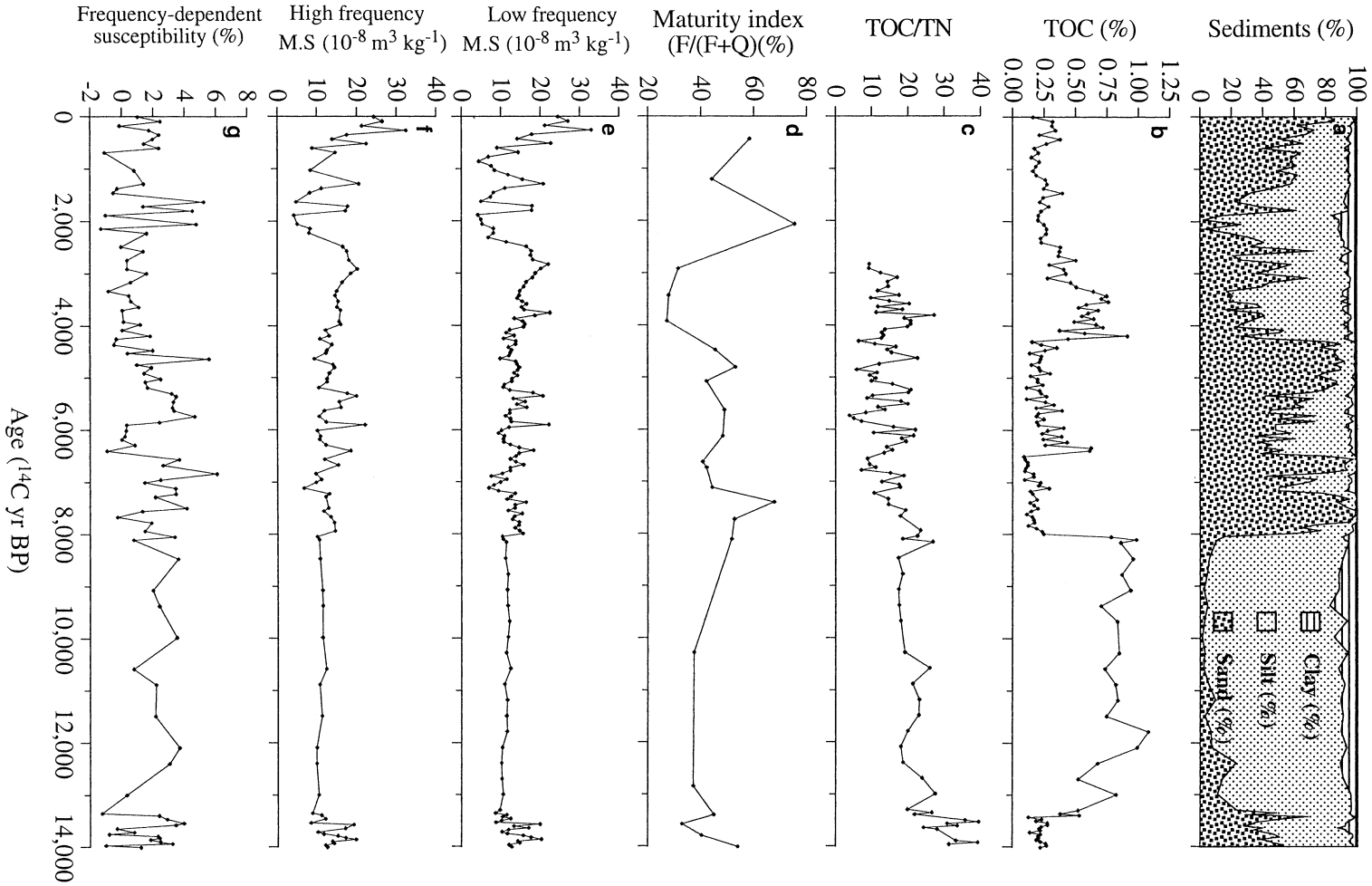


Fig. 3. Secular variations in proxies in Lake Yanhaizi. (a) Sediment composition, (b) TOC, (c) TOC/TN, (d) maturity index, (e) low-frequency magnetic susceptibility, (f) high-frequency magnetic susceptibility, and (g) frequency-dependent susceptibility.

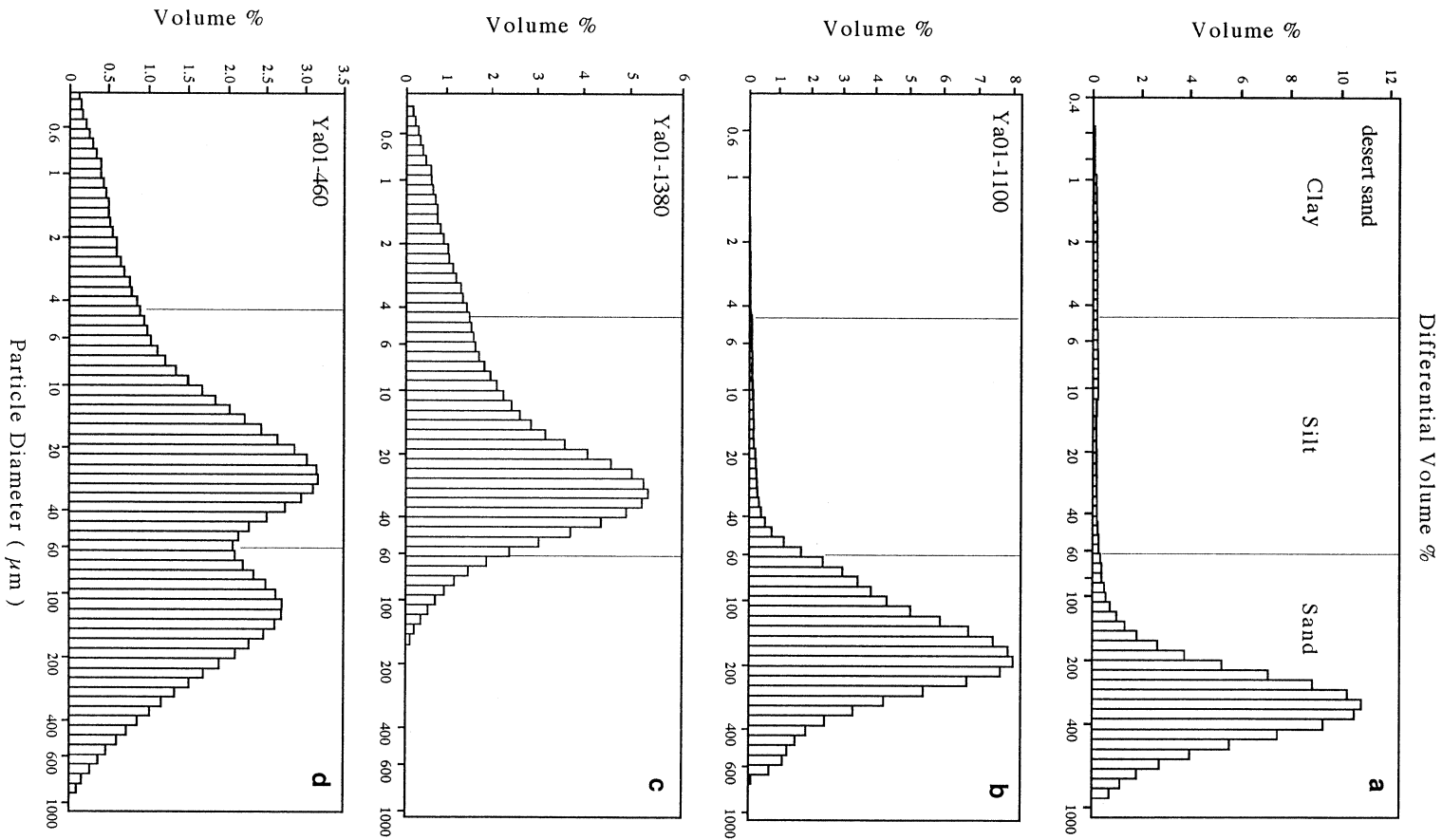


Fig. 4. Volumetric particle size distributions for (a) desert sand sampled nearby, and samples at depth (b) 1100, (c) 1380, and (d) 460 cm in Core YA01.

(Hsu, 1989). While we did not calibrate the integrated area of the 2-theta to intensity plot of feldspars and quartz to their actual concentrations here, we directly used the integrated area to calculate the maturity indices. Only 23 samples were analyzed, but the higher values generally occur in the dry segments (Fig. 3e). As a rule, a higher maturity index indicates that the deposited sediments had undergone low-extent chemical weathering in drier environments; on the other hand, a lower index indicates that the deposited sediments had undergone higher-extent chemical weathering in more humid environments (Hsu, 1989). Therefore, the higher maturity indices in the mid-Holocene supports the notion of a drier climate reconstructed from other proxies. The interpretation of the maturity index to the humidity of the environment is, of course, true only when there is no variation in the mineral composition of the provenance of dust and dune sand. Indeed, Wen (1990) has shown that both the mineralogy and chemical composition of regolith materials contributed to the Loess Plateau having very little variation across the whole of northern China.

Fig. 3e,f reveal the coherent variations in low-frequency (Lf) and high-frequency (Hf) magnetic susceptibilities. The susceptibilities within the core fluctuate between $4.2 \times$ and $33 \times 10^{-8} \text{ m}^3 \text{ kg}^{-1}$, with the highest values during the last 500 yr. Qualitatively, these variations seem to correlate with the abundance of sand content (Fig. 3a). Frequency-dependent susceptibility (F.D.S.), defined as $\{[(Lf-Hf)/Lf] \times 100\%$, falls below 6% and shows only minor variability over the past 14 kyr BP (Fig. 3g). According to Evans and Rokoosh (2000), the F.D.S. typically falls within the range of 0–4% for completely unweathered, or only slightly weathered, parental loess, whereas well-developed soils yield values between 8% and 12%. Thus, the low F.D.S. indicates that the sediments of our study area have undergone only insignificant soil development, which is in accordance with the low TOC values throughout the core. Magnetic susceptibility in our study area must have been controlled by different mechanisms than those related to loess and paleosol. However, without further analysis of mineralogy and other magnetic parameters, it can only be

concluded that the samples are only slightly weathered.

5. Discussion

5.1. Dry Holocene Megathermal in Inner Mongolia

Sections where coarse sediment dominates (Fig. 3a) show similar sedimentary textures to those of the nearby dune sands and have high maturity indices (Fig. 3d) but low organic carbon contents (Fig. 3c); thus, they denote arid environments. On the other hand, finer sediments with high organic contents and low maturity indices imply that these sediments were actually deposited in a humid environment. Three humid phases, 13.4–8.0, 6.4–5.8 and 4.3–3.2 kyr BP, were identified, with the first phase the wettest and the third the second wettest. The Holocene Megathermal appears to be arid. The first wet phase, which started at 13.4 kyr BP, denotes the onset of the last deglaciation (The European Bølling–Allerød interstadial), which is characterized by warmer, wetter conditions resulting in an increase in vegetation covering in Inner Mongolia (Zhou et al., 1996). This 13.4–8.0 kyr BP humid episode roughly corresponds to the monsoon maximum which occurred in countries that encompass the Arabian Sea between about 7850–8850 and about 11 300 yr BP (Sirocko et al., 1993). It may also be supported by the postulated low-latitude vegetation development as based on the observation of a period of prominent high atmospheric methane concentration in the early Holocene (Blunier et al., 1995).

Hafsten (1970) proposed the term ‘Megathermal’ to represent the warmest period from 8.2 to 3 cal. kyr BP since the Last Glacial Maximum. The GRIP ice core isotope records also reflect higher optimum temperatures for the Holocene between ca. 8.6 and 4.3 cal. kyr BP (Johnsen et al., 2001). In eastern Asia, paleotemperatures derived from sporopollen assemblages in the eastern part of Hebei Province (Shi et al., 1994) and on the Loess Plateau (Sun and Zhao, 1991) also show that the Holocene Megathermal was the warmest in the Holocene (Fig. 5a,b).

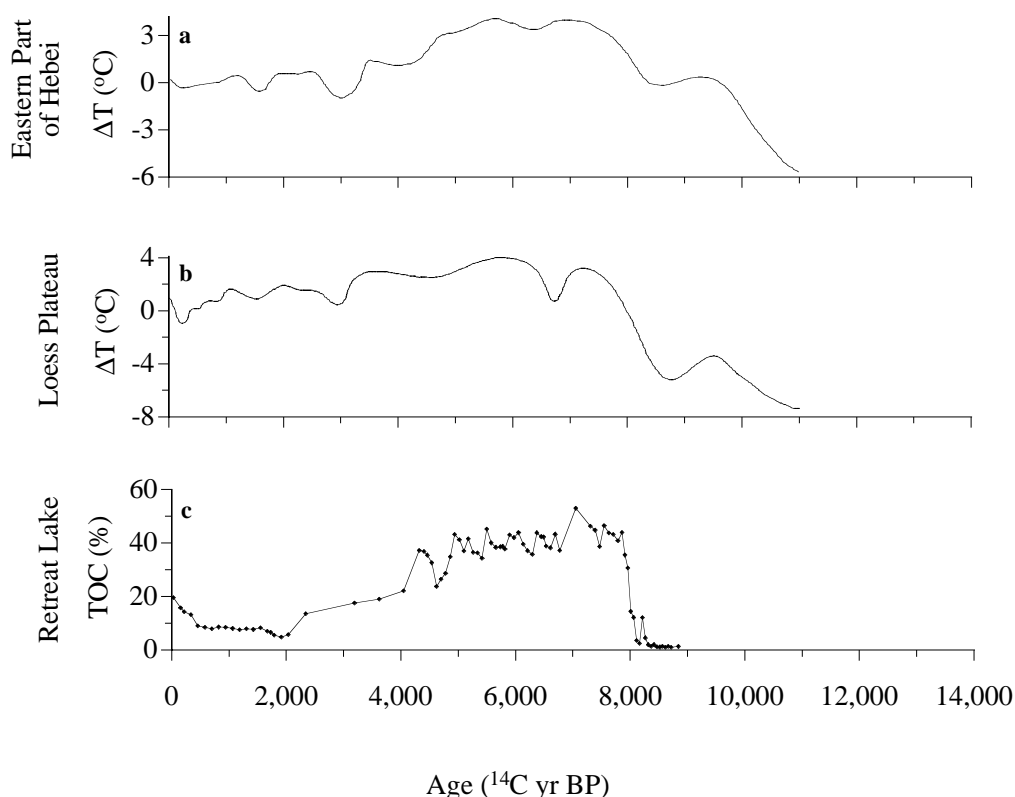


Fig. 5. Sporopollen assemblages derived temperature differences ΔT ($T - T_{\text{average}}$) in (a) the eastern part of Hebei Province (Shi et al., 1994) and (b) the Loess Plateau (Sun and Zhao, 1991). (c) Variations in the TOC (%) in Retreat Lake.

In order to clarify whether the paleoenvironment record obtained at Lake Yanhaizi is a local signal or a regional record, here we compare our results with other proxy records at the periphery of the summer monsoon-influenced areas. From variations in pollen concentration and organic carbon content, Zhou et al. (1996) found that there was a dry phase from 7.5 to 3.5 kyr BP in the Midiwan profile, 250 km south of Lake Yanhaizi (Fig. 1a). A relatively arid climate was also reported from 7 to 5.6 kyr BP in the Tengger Desert (Guo et al., 2000), 300–600 km west of Lake Yanhaizi. Further, after the increase of aeolian material at ca. 6.9 kyr BP, arid and deteriorating conditions were reconstructed and were determined to range between 5.6 and 4.5 kyr BP in the Dali Nor area (Haoluku, 116°45'E, 42°57'N, 1295 m a.s.l.), and to have been followed by a minor amelioration at 4.5–3.0 kyr BP (Wang et al., 2001). In addition, the water level of Dali Nor

Lake (116°30'E, 43°20'N) began to drop as early as ca. 7 kyr BP (Geng and Zhang, 1988). Persistent arid climate from 8 to 3 kyr BP was also inferred from Core QH85-14C, drilled in Qinghai Lake (An et al., 2000). A striking abundance of deciduous broad-leaf pollen occurred from 11 to 8 kyr BP, implying late Pleistocene and early Holocene maximum monsoon precipitation. A second humid epoch occurred between 1.6 and 2.5 kyr BP. After 1.5 kyr BP, the percentage of broad-leaf pollen rose to 30%, but this may have been due to human perturbations. Paleoclimate records from Badain Jaran and Tengger deserts further west indicated that the first humid impulse after a long-term aridity occurred between 12 and 13 kyr BP but it was again generally dry between 32 and 10 kyr BP (Pachur et al., 1995; Rhodes et al., 1996; Wünnemann and Pachur, 1998).

For the Younger Dryas period, our records show that it was wet in Lake Yanhaizi (Fig. 3).

This is contrary to the notion that a cold climate has always been accompanied by a dry climate in east China (An, 2000). This may be due to the insensitivity of our study area. As a result, our record does not show the rapid transitions from dry to humid and back to dry climatic conditions recorded in the Midiwan profile (Zhou et al., 1996; Zhou et al., 1999) during the Younger Dryas. Alternatively, this may be a result of different controlling climate systems at these two places. For example, it was reported to be humid in western Tibet and at the northern and north-eastern margins of the Tibetan Plateau during the Younger Dryas (Lehmkuhl, 1997; Lehmkuhl and Haselein, 2000). There is also still no evidence of a glacier advance in High Asia during the Younger Dryas because of an intensified summer monsoon (Lehmkuhl, 1997).

Synchronous changes in several past records reconstructed for the northern limit of the summer monsoon may reflect regional changes in effective humidity (precipitation minus evaporation). The data here clearly indicate that the Holocene Megathermal was an arid period in the northern limit of the summer monsoon. This is in direct contrast to the humid phenomenon reported elsewhere in China and to the previously presumed notion that the northern limit of the summer monsoon moved landward during this period (Shi et al., 1994).

To illustrate this point, the high TOC content at Retreat Lake in Taiwan, taken as a wet signal (Chen et al., 2003), is almost the mirror image of the TOC signal in Lake Yanhaizi where low TOC is taken as a reflection of low humidity (Fig. 5c). This is evidence that the Holocene Megathermal started at 8 kyr BP but began to cool at 4 kyr BP. Sun et al. (1998a) reported that sandy loam soils were widely developed in the eastern part of northern China as a result of increased monsoonal precipitation between 9.0 and 3.0 kyr BP, broadly coincident with the Holocene Optimum. Similarly, magnetic susceptibility of the Baxie loess profile delineated a humid episode from 9.7 to 5.3 kyr BP (An et al., 1993). A compilation of pollen-based biome reconstruction shows a northwest shift of forest zones (increased annual moisture availability) in China at 6 kyr BP and

this is possibly on account of direct radiative effects which produced a stronger-than-present summer monsoon (Yu et al., 1998, 2000). It is evident that the Holocene Megathermal was warm and generally wet in eastern China (Shi et al., 1993) and Taiwan. However, it was arid in Inner Mongolia.

It has been reported that the fossil extents of the sandy deserts in China during the Holocene Optimum contracted and retreated to the west of Helan Mountain (Sun et al., 1998a); however, based on our reconstruction, the sandy desert in Inner Mongolia actually expanded during the mid-Holocene. Nevertheless, previous studies have made few specific comments on the paradox that the warmest Holocene Megathermal did not result in wet conditions in all of these areas. The nature and timing of the Holocene climate changes, therefore, have long bewildered scientists studying eastern Asia.

5.2. Possible mechanism

In order to interpret an asynchronous Holocene Optimum phenomenon in East Asia, An et al. (2000) proposed a progressive weakening of the summer monsoon as the summer solar radiation anomaly decreased progressively and the East Asian monsoon index declined through the Holocene. An et al. (2000) defined the Holocene Optimum as an effective moisture maximum, without making reference to temperature. However, some of An et al.'s records do not show an earlier maximum humidity during 10–8 kyr BP, but instead, their Baxie and Weinan loess profiles indicate that the optimum occurred during the mid-Holocene rather than the early Holocene (An et al., 2000). Wang et al. (1999) reported a Termination I and early Holocene humidity maximum event in the South China Sea based on a paleosalinity reconstruction and the concurrent presence of a higher fluvial input of mud which may point to a humid condition in south China. This also contradicts the notion of an asynchronous Holocene Optimum whereby the maximum humidity occurred in 3.0 kyr BP in south China (An et al., 2000).

Guo et al. (2000) found a prolonged, somewhat drier interval during the mid-Holocene in north-

ern Africa and China. Further work points to a drier 6 kyr BP in south China (Zhengtang Guo, private communication, 2000). What these authors adopted to justify the mid-Holocene dryness is the notion of a mechanism which involved a general weakening of the monsoons, with the drier climate in the monsoonal area extending in a broad geographic realm from northern Africa to eastern China (Guo et al., 2000). But, there are indeed records showing a humid Megathermal, such as in the loess profiles denoted by higher magnetic susceptibility (An et al., 1993, 2000) and in the TOC record of Retreat Lake (Fig. 5c). Also, other than the oceanic patterns that Guo et al. (2000) cited, there are warmer sea-surface temperatures reconstructed from foram abundances of high-resolution cores retrieved in the Okinawa Trough and South China Sea (Jian et al., 1996).

The dry Holocene Megathermal in Inner Mongolia may also be elucidated by monsoon dynamics. These require that increased atmospheric convergence and rising motion (and hence increased monsoon precipitation) are balanced by increased upper-level divergence and subsidence (and hence decreased precipitation). In relatively simple monsoon systems, such as the American monsoon, the geographic relationship between the zones of convergence and of subsidence are relatively straightforward and give rise to observed bi-polar (wetter/drier) patterns in precipitation anomalies. The situation in Asia is more complex, however, because of the interplay between the Pacific, India and the East African monsoon systems and because of the strong influence of the so-called winter monsoon. Nevertheless, it is clear that increases in the extent of the monsoon during the Holocene were accompanied by decreased precipitation in zones around the core region of the expanded monsoon (Sandy P. Harrison, private communication, 2001).

It is argued here, however, that the discrepancy was more likely to have been due to the greatly enhanced rate of evaporation than to the higher monsoon precipitation in Inner Mongolia. This would have reduced the effective humidity in the warm, arid climate near the northern boundary of the summer monsoon. This explanation would account for the fact that the highest temperatures

in the Holocene Megathermal, as revealed in the eastern part of Hebei Province (Shi et al., 1994; Fig. 5a), the Loess Plateau (Sun and Zhao, 1991; Fig. 5b), the Okinawa Trough and the northern South China Sea (Fig. 6a–c), correlate well with the dry phases in Inner Mongolia. Conversely, the 4.3–3.2-kyr BP coldest period in the Holocene corresponds with a wet phase in Inner Mongolia when evaporation decreased as temperature dropped. This also contradicts previous suggestions that increased evaporation due to the temperature maximum at 6000 yr BP was unable to overcompensate for the intensified precipitation, hence making it become wetter (Sarnthein, 1978).

Fig. 7 shows the monthly precipitation (P) and evaporation (E) at weather stations in Hunjinchi and Daihai. Data for 1971–1980 for Hunjinchi, located near Lake Yanhaizi, are plotted (data were provided by the station). Indeed, the higher the temperature, the higher the precipitation. Although this was accompanied by a greater increase in evaporation, the rate of increase in evaporation was much higher, resulting in a higher $E-P$ at higher temperatures. The resulting higher $E-P$ at higher temperatures may account for the fact that the effective humidity was lower during the Holocene Megathermal in Inner Mongolia.

Faced with the increasing trend in temperature due to global warming (Mann et al., 1998; Shi et al., 1999), there is another way, based on lake-level fluctuations, to assess the hypothesis that in the future the northern border of monsoon-influenced areas will become drier as it gets warmer. Although no long-term lake-level observations are available for Lake Yanhaizi, the observed lake-level fluctuations in Qinghai Lake, 800 km to the southwest (Fig. 1a), have shown a decreasing trend since the early 1900's (Qin and Huang, 1998). Lake water balance studies for the 1958–1990 period demonstrate that evaporation exceeded water input (precipitation plus runoff), resulting in lower lake levels (Qin and Huang, 1998). A similar trend with respect to lower lake levels since 1960 has been monitored in Lake Daihai (Wang and Feng, 1992), and the data from a nearby weather station, Liancheng, has the same P , E as well as $E-P$ vs. temperature relationships (Fig. 7c,d) as that of the weather station near

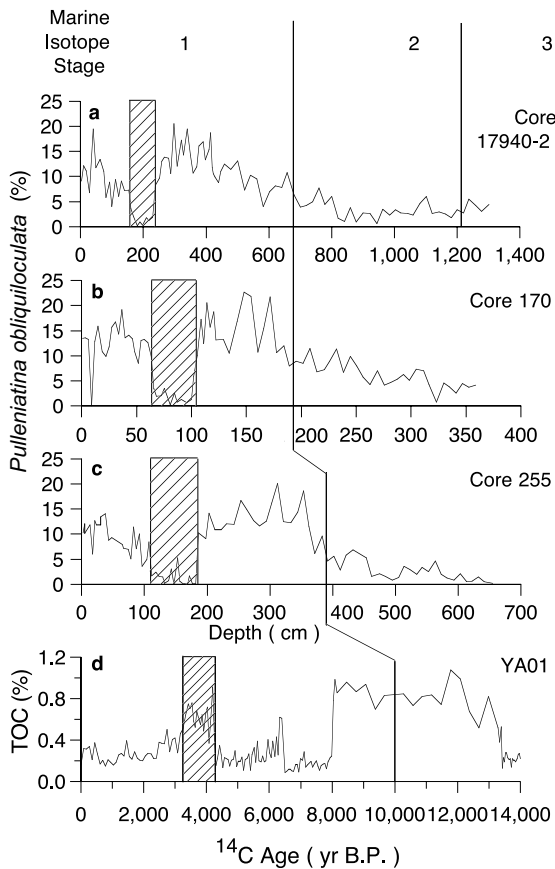


Fig. 6. Variations in *Pulleniatina obliquiloculata* (%) in cores taken from (a) the South China Sea (Core 17940-2; Jian et al., 1996) and (b,c) the Okinawa Trough (Cores 255 and 170; Li et al., 1997) and (d) their correlation with TOC (%) records in Lake Yanhaizi. The vertical lines connecting the panels indicate places where the ^{14}C age is 10 kyr BP, and the numbers at the top of the first panel denote the marine isotope stages. The hatched areas denote the *Pulleniatina* Minimum Event.

Lake Yanhaizi. With global warming, the climate may indeed bring about greater evaporation and an overall drier environment in Inner Mongolia.

5.3. Correlation with marine records

Pulleniatina obliquiloculata is a tropical planktonic foraminifer living primarily in a narrow belt between about 10°N and 10°S , and is very sensitive to winter temperature (Li et al., 1997).

Variations in *P. obliquiloculata* in the Okinawa Trough (Core 255, $123^{\circ}07'\text{E}$, $25^{\circ}12'\text{N}$, w.d. 1575 m; Core 170, $125^{\circ}48'\text{E}$, $26^{\circ}38'\text{N}$, w.d. 1470 m; Jian et al., 1996; Li et al., 1997; Ujiie and Ujiie, 1999) and the South China Sea (Core 17940, $117^{\circ}25'\text{E}$, $20^{\circ}07'\text{N}$, w.d. 1727 m; Jian et al., 1996) indicate that this warm-water species was low in abundance around 10 kyr BP but that it abruptly increased in abundance about 7 kyr BP just prior to showing a drastic decrease from 4360 to 3260 yr BP (Fig. 6a–c). This 4.3–3.2 kyr BP decline, known as the *Pulleniatina* Minimum Event (Jian et al., 1996; Li et al., 1997; Ujiie and Ujiie, 1999; Wang et al., 1999), may be indicative of cooling winter sea-surface temperatures (Jian et al., 1996; Li et al., 1997). Analysis of coccolith (*Florisphaera profunda*) records have confirmed this (Cheng and Wang, 1998). Wei et al. (1997) also found that nannofossil preservation improved during these periods, probably reflecting a local cooling event. They further reported that the relative content of *F. profunda* had the same distribution as *P. obliquiloculata* in the South China Sea.

The *Pulleniatina* Minimum Event around 4 kyr BP along with the paucity of the species around 10 kyr BP corresponded to the two wet phases around 4 and 10 kyr BP found at Lake Yanhaizi (Fig. 6). It was also found in Retreat Lake that there was a hiatus possibly due to the total drying out of the lake between 3.9 and 2.1 cal. kyr BP (Chen et al., 2003; Fig. 5c). The cooling event has also been deduced from coral Sr/Ca ratios and lake sediments at other localities in Taiwan (Liew and Hsieh, 2000), and possibly correlate to the late Holocene neoglaciation registered as a glacier advance in the Tibetan Plateau (Lehmkuhl, 1997). On the other hand, the high abundance '*P. obliquiloculata* maximum' corresponded to the dry phase between 4.2 and 8 kyr BP at Lake Yanhaizi (Fig. 6) and the humid phase between 8.0 and 4.2 kyr BP in Retreat Lake (Fig. 5c), signaling two contrasting scenarios in Inner Mongolia and eastern China through the Holocene climate variation. The mid-Holocene Megathermal also correlates with the disappearance of *Globorotalia truncatulinoides* from the cores of the South China Sea and Okinawa Trough between 8

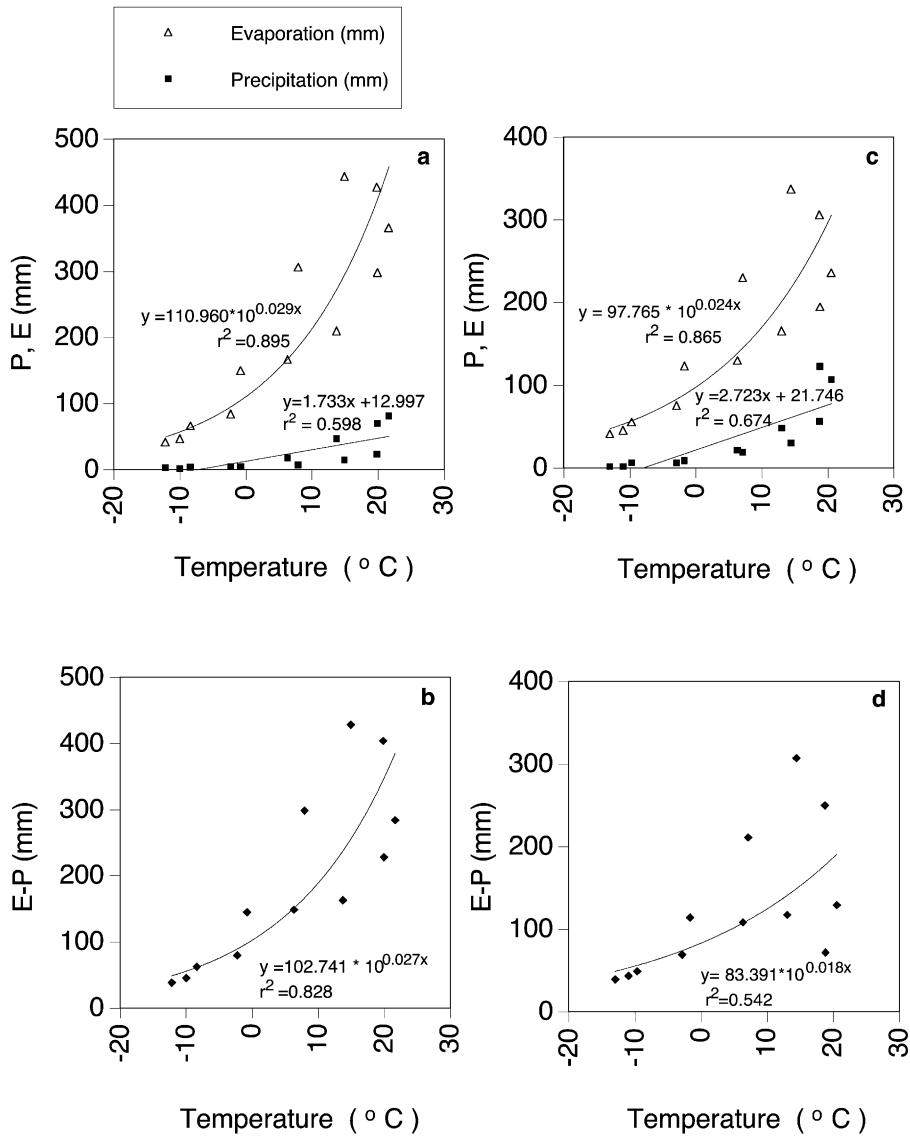


Fig. 7. (a) Average monthly precipitation (P) and evaporation (E). (b) $E-P$ vs. temperature between 1971 and 1980 at the Hang-jienqi weather station. (c) P and E . (d) $E-P$ vs. temperature between 1959 and 1988 at the Liancheng weather station located near Lake Daihai (Wang and Feng, 1992).

and 4 cal. kyr BP, which indicates a mid-Holocene reduction in the thickness of the North Pacific subtropical mode water thermostad in the western North Pacific (Jian et al., 2000).

Kim and Kennett (1998) have shown the Holocene marine transgression in the Yellow Sea occurred between 11.3 and 7 kyr BP based on

benthic foraminiferal and stable isotopic data, while on the west coast of Korea, the marine transgression started at 13 kyr BP (Park et al., 1994). This transgression correlates not only with the first humid phase in Lake Yanhaizi, but also with the humidity maximum during 15–9 cal. kyr BP in the South China Sea (Core 17940,

117°25'E, 20°07'N, w.d. 1727 m; Wang et al., 1999). It is suggested that such good correlations in climate changes over such a wide geographical distribution both on land and in the ocean are highly indicative that land and the ocean interacted.

5.4. Aeolian dust records

Due to its dryness and proximity to the Gobi Desert – thought to be the major source of dust in the Greenland ice cores (Biscaye et al., 1997) – Inner Mongolian lakes provide an excellent setting with which to examine paleoenvironmental changes, especially those involving the long-range transport of aeolian dusts. Liu (1985) stated that the paucity or absence of silt in the desert sand dunes is not unexpected in the deserts northwest of the Loess Plateau, implying that silts – as an abrasion product of sand dune terrain – are readily lost by deflation, leaving only sands in the source area. Recent field observations indicate that the silt-rich alluvial fan systems in the Hexi Corridor region (between the Tengger Desert and Loess Plateau) have supplied a considerable amount of material to the loess columns of that region (Derbyshire et al., 1998). Variations of aeolian silt flux in downwind sink areas can thus serve as a gauge of source area conditions.

Periods of higher aeolian flux in the GISP2 ice core (O'Brien et al., 1995; Fig. 8a) are found to correlate with lesser amounts of sediments finer than 50 µm (Fig. 8b), which are the basic fraction of wind-blown dusts (Liu, 1985) in our study area (clay accounts for a negligible amount as compared to silt and sand) and corresponds to dry periods in Lake Yanhaizi (Fig. 8c). This is possibly evidence of a teleconnection in climate systems between East Asia and polar, high-latitude areas.

In most studies, an increase in dust accumulation has been regarded as an indicator of increased aridity in the interior of Asia (Nilson and Lehmkuhl, 2001; Rea, 1994; Rea and Leinen, 1988). The atmospheric circulation modes in eastern Asia are long-distance dust transport via upper-level westerly winds along with strong vertical air motions which incorporate dust into the

Westerly Jet over Inner Asia during interglacial times, and low-level Eastern Asian winter monsoon, which prevailed during Glacial times (Pye and Zhou, 1989). But it has long been problematic that maximum dust flux to the North Pacific has been recorded in the mid-Holocene (Rea and Leinen, 1988; Wang et al., 1998), while Holocene rates of loess accumulation on the Loess Plateau have been low (Pye and Zhou, 1989).

Because no evidence of arid mid-Holocene conditions has been reported for the early 1990s, Pye and Zhou (1989) had to invoke different patterns of atmospheric circulation to explain the differences in the timing of the dust flux maximum between the continent and the North Pacific where dust originates mainly from Inner Asia. It is, however, now clear that the arid Holocene Megathermal in Inner Mongolia may easily account for the greatly increased dust flux found in the North Pacific. Silt content was indeed lower or even absent during this period in Lake Yanhaizi (Fig. 3a). Relatively higher dust deposition rates in the central Loess Plateau were also found during 10–5 kyr BP in the Holocene epoch (An, 2000). Besides, in the wake of a higher fluvial input of mud during Termination I and the early Holocene, there was indeed a period characterized by higher contents of silt in the two South China Sea cores, 17940-1/2 and 17939-2, (Wang et al., 1999). To summarize, the Asian winter monsoon transports dusts from their source area in Inner Mongolia to Lake Yanhaizi and the Loess Plateau and, finally, to the South China Sea and the North Pacific. A dry mid-Holocene in Lake Yanhaizi corresponds to a higher dust deposition rate in the downwind regions.

6. Conclusions

Preliminary evidence from a sediment core collected from Lake Yanhaizi in Inner Mongolia indicates that three humid phases, 13.4–8.0, 6.4–5.8 and 4.3–3.2 kyr BP, have occurred since 14 kyr BP. Notwithstanding this fact, in general, the Holocene Megathermal was marked by relative dryness. This is in complete agreement with findings noted in the arid–semiarid zones elsewhere in In-

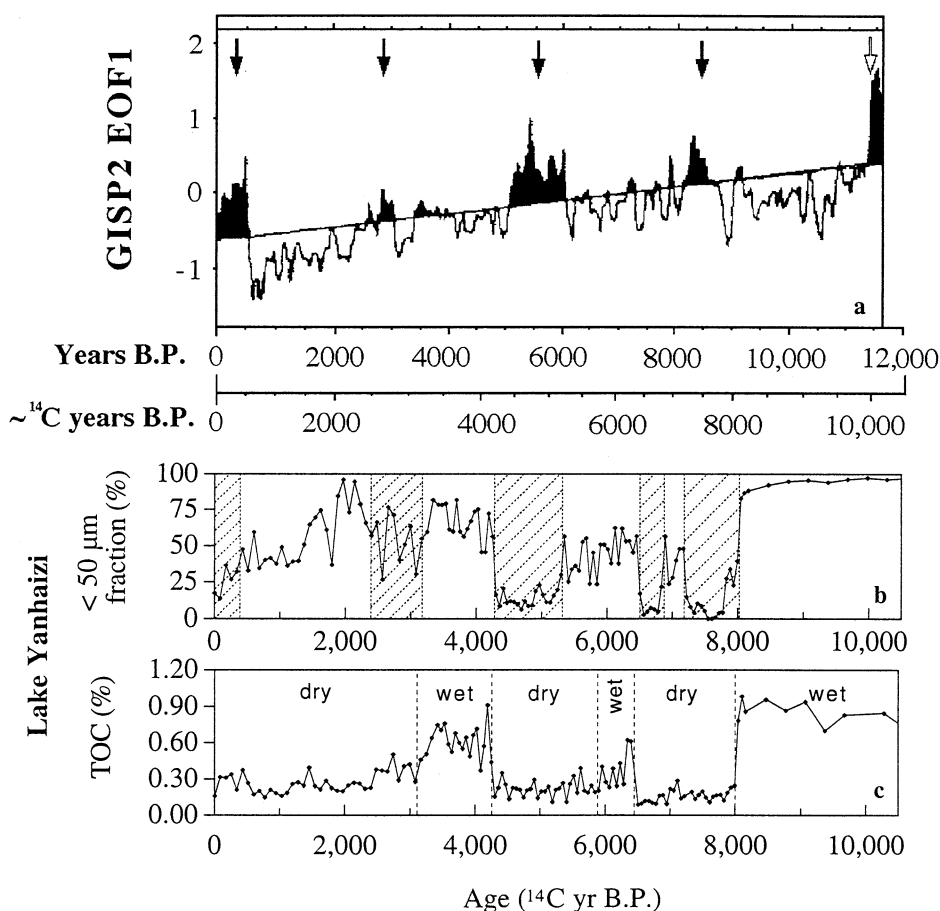


Fig. 8. (a) First and dominant empirical orthogonal function (EOF1), quantifying common behavior among Holocene glaciochemical species in the GISP2 ice core (O'Brien et al., 1995). Arrows pointing to the major positive EOF1 deviation periods denote a higher influx of marine sea salt and terrestrial dusts. (b) Contents of grain size less than 50 μm . (c) Environmental conditions represented by the TOC of Lake Yanhaizi.

ner Mongolia, but it is contrary to the humid Holocene Megathermal found elsewhere in China and Taiwan. The reason for this may be that much enhanced evaporation over higher monsoon precipitation at Lake Yanhaizi reduced effective humidity. The dry (warm) Holocene Megathermal at Lake Yanhaizi also corresponds to the high temperatures found in the Okinawa Trough and the South China Sea, and provides direct evidence for the missing source of aeolian dust in the North Pacific. Such correlations may very well be indicative of the influence of the Asian monsoon which is associated with the global atmospheric circulation system.

Acknowledgements

We are indebted to Prof. K.J. Hsu for his encouragement, and Ms. H.I. Huang and Mr. I. Hsu for their assistance with the field work. We also wish to thank Prof. Yu-Chia Chung, Dr. Chung-Ho Wang, Dr. Peter B. Yuan, Mrs. H.Y. Li and Mrs. K.H. Chen for their assistance with the analyses. Drs. P. De Deckker, J. Bloemendal, F. Lehmkuhl, J. Dobson, Z.T. Guo and S. Harrison helped to strengthen an earlier version of the manuscript. This work was financially supported by grant NSC90-2611-M-110-006 from the National Science Council of the ROC.

References

- An, Z.S., 2000. The history and variability of the East Asian palaeomonsoon climate. *Quat. Sci. Rev.* 19, 171–187.
- An, Z.S., Liu, T.S., Lu, Y.C., Porter, S.C., Kukla, G.J., Wu, X.H., Hua, Y.M., 1990. The long-term paleomonsoon variation recorded by the loess-paleosol sequence in central China. *Quat. Int.* 7/8, 91–95.
- An, Z.S., Porter, S.C., Zhou, W.J., Lu, Y.C., Donahue, D.J., Head, M.J., Wu, X.H., Ren, J.Z., Zheng, H.B., 1993. Episode of strengthened summer monsoon climate of Younger Dryas age on the Loess Plateau of central China. *Quat. Res.* 39, 45–54.
- An, Z.S., Porter, S.C., Kutzbach, J.E., Wu, X.H., Wang, S.M., Liu, X.D., Li, X.Q., Zhou, W.J., 2000. Asynchronous Holocene optimum of the East Asian monsoon. *Quat. Sci. Rev.* 19, 743–762.
- Bernasconi, S.M., Dobson, J., Mckenzie, J.A., Ariztegui, D., Niessen, F., Hsu, K.J., Chen, Y., Yang, Q., 1997. Preliminary isotopic and paleomagnetic evidence for Younger Dryas and Holocene climate evolution in NE Asia. *Terra Nova* 9, 246–250.
- Biscaye, P.E., Grousset, F.E., Revel, M., Van der Gaast, S., Zielinski, G.A., Vaars, A., Kukla, G., 1997. Asian provenance of glacial dust (stage 2) in the GISP2 ice core, Summit, Greenland. *J. Geophys. Res.* 102 (C12), 26675–26781.
- Blunier, T., Chappellaz, J., Schwander, J., Stauffer, B., Raynaud, D., 1995. Variations in atmospheric methane concentration during the Holocene epoch. *Nature* 374, 46–49.
- Chen, C.T.A., Wann, J.K., Lou, J.Y., 2001. Aeolian flux of metals in Taiwan in the past 2600 years. *Chemosphere* 43, 287–294.
- Chen, C.T.A., Wann, J.K., Lou, J.Y., 2003. High resolution paleoclimatic records in Taiwan, submitted.
- Cheng, X.R., Wang, P.X., 1998. Variations in Late Quaternary upper ocean structure of Okinawa Trough – a nannofossil approach. *Sci. China (Ser. D)* 41, 290–296.
- COHMAP Members, 1988. Climatic changes of the last 18,000 years: observations and model simulations. *Science* 241, 1043–1052.
- Derbyshire, E., Meng, X.M., Kemp, R.A., 1998. Provenance, transport and characteristics of modern aeolian dust in western Gansu Province, China, and interpretation of the Quaternary loess record. *J. Arid Environ.* 39, 497–516.
- Ding, Z.L., Sun, J.M., Rutter, N.W., Rokosh, D., Liu, T.S., 1999. Changes in sand content of loess deposits along a north-south transect of the Chinese Loess Plateau and the implications for desert variations. *Quat. Res.* 52, 56–62.
- Enzel, Y., Ely, L.L., Mishra, S., Ramesh, R., Amit, R., Lazar, B., Rajaguru, S.N., Baker, V.R., Sandler, A., 1999. High-resolution Holocene environmental changes in the Thar Desert, Northwestern India. *Science* 284, 125–128.
- Evans, M.E., Rokosh, C.D., 2000. The last interglacial in the Chinese Loess Plateau: a petromagnetic investigation of samples from a north-south transect. *Quat. Int.* 68-71, 77–82.
- Fryberger, S.G., Al-Sari, A.M., Clisham, T.J., 1983. Eolian dune, interdune, sand sheet, and siliclastic sabkha sediments of an offshore prograding sand sea, Dhahran Area, Saudi Arabia. *AAPG Bull.* 67, 280–312.
- Gao, Y.X., 1962. On some problems of Asian monsoon. In: Gao, Y.X. (Eds.), *Some Questions About the East Asian Monsoon*. Science Press, Beijing, pp. 1–49.
- Geng, K., Zhang, Z., 1988. Geomorphologic features and evolution of the Holocene lakes in Dali Nor Area, the Inner Mongolia (in Chinese). *J. Beijing Normal Univ. (Nat. Sci.)* 4, 94–100.
- Guo, Z.T., Petit-Maire, N., Kröpelin, S., 2000. Holocene non-orbital climatic events in present-day arid areas of northern Africa and China. *Glob. Planet. Change* 26, 97–103.
- Hafsten, U., 1970. A sub-division of the Late Pleistocene period on a synchronous basis, intended for global and universal usage. *Palaeogeogr. Palaeoclimatol. Palaeoecol.* 7, 279–296.
- Hsu, K.J., 1989. *Physical Principles of Sedimentology: A Readable Textbook for Beginners and Experts*. Springer, Berlin.
- Hung, G.W., Chung, Y.C., 1998. Particulate fluxes, ^{210}Pb and ^{210}Po measured from sediment trap samples in a canyon off northeastern Taiwan. *Cont. Shelf Res.* 18, 1475–1491.
- Janitzky, P., 1987. Particle size analysis. In: Singer M. and P. Janitzky (Eds.), *Field and Laboratory Procedures Used in Soil Chrono-sequence Study*. USGS Bull. 1648, 11–16.
- Jian, Z.M., Li, B.H., Pflaumann, U., Wang, P.X., 1996. Late Holocene cooling event in the western Pacific. *Sci. China (Ser. D)* 39, 543–550.
- Jian, Z.M., Li, B.H., Huang, B.Q., Wang, J.L., 2000. Globorotalia truncatulinoides as indicator of upper-ocean thermal structure during the Quaternary: evidence from the South China Sea and Okinawa Trough. *Palaeogeogr. Palaeoclimatol. Palaeoecol.* 162, 287–298.
- Johnsen, S.J., Dahl-Jensen, D., Gundestrup, N., Steffensen, J.P., Clausen, H.B., Miller, H., Masson-Delmotte, V., Sveinbjörnsdóttir, A.E., White, J., 2001. Oxygen isotope and paleotemperature records from six Greenland ice-core stations: Camp Century, Dye-3, GRIP, GISP2, Renland and NorthGRIP. *J. Quat. Sci.* 16, 299–307.
- Kim, J.M., Kennett, J.P., 1998. Paleoenvironmental changes associated with the Holocene marine transgression, Yellow Sea (Hwanghae). *Mar. Micropaleontol.* 34, 71–89.
- Kukla, G., Heller, F., Liu, X.M., Xu, T.C., Liu, T.S., An, Z.S., 1988. Pleistocene climates in China dated by magnetic susceptibility. *Geology* 16, 811–814.
- Kutzbach, J., Otto-Bliessen, B.L., 1982. The sensitivity of the African-Asian monsoonal climate to orbital parameter changes for 9, 000 yr BP in a low-resolution general circulation model. *J. Atmos. Sci.* 39, 1177–1188.
- Kutzbach, J.E., Street-Perrott, F.A., 1985. Milankovitch forcing of fluctuations in the level of tropical lakes from 18 to 0 kyr BP. *Nature* 317, 130–134.
- Kutzbach, J., Bonan, G., Foley, J., Harrison, S.P., 1996. Vegetation and soil feedbacks on the response of the African monsoon to orbital forcing in the early to middle Holocene. *Nature* 384, 623–626.

- Lehmkuhl, F., 1997. Late Pleistocene, Late-Glacial and Holocene glacier advances on the Tibetan Plateau. *Quat. Int.* 38/39, 77–83.
- Lehmkuhl, F., Haselein, F., 2000. Quaternary paleoenvironmental change on the Tibetan Plateau and adjacent areas (West China and Mongolia). *Quat. Int.* 65/66, 121–145.
- Li, B.H., Jian, Z.M., Wang, P.X., 1997. Pulleniatina obliquiloculata as a paleoceanographic indicator in the southern Okinawa Trough during the last 20,000 years. *Mar. Micro-paleontol.* 32, 59–69.
- Li, B.S., Zhang, D.D., Jin, H.L., Wu, Z., Yan, M.C., Sun, W., Zhu, Y.Z., Sun, D.H., 2000. Paleo-monsoon activities of Mu Us Desert, China since 150 ka B.P. – a study of the stratigraphic sequences of the Milanggouwan Section, Salawusu River area. *Palaeogeogr. Palaeoclimatol. Palaeoecol.* 162, 1–16.
- Liew, P.M., Hsieh, M.L., 2000. Late Holocene (2 ka) sea level, river discharge and climate interrelationship in the Taiwan region. *J. Asian Earth Sci.* 18, 499–505.
- Liu, T.S., 1985. *Loess and the Environment*. China Ocean Press, Beijing.
- Lou, J.Y., Chen, C.T.A., 1997. Paleoclimatological and paleoenvironmental records since 4000 a BP. in sediments of alpine lakes in Taiwan. *Sci. China (Ser. D)* 40, 424–431.
- Lou, J.Y., Chen, C.T.A., Wann, J.K., 1997. Paleoclimatological records of the Great Ghost Lake in Taiwan. *Sci. China (Ser. D)* 40, 284–292.
- Mann, M.E., Bradley, R.S., Hughes, M.K., 1998. Global-scale temperature patterns and climate forcing over the past six centuries. *Nature* 392, 779–787.
- Meyers, P.A., 1997. Organic geochemical proxies of paleoceanographic, paleolimnologic, and paleoclimatic processes. *Org. Geochem.* 27, 213–250.
- Nemoto, M., Ohkuro, T., Xu, B., 1997. The role of weed invasion in controlling sand dune reactivation in abandoned fields in semi-arid Inner Mongolia. *China Ecol. Res.* 12, 325–336.
- Nilson, E., Lehmkuhl, F., 2001. Interpreting temporal patterns in the late Quaternary dust flux from Asia to the North Pacific. *Quat. Int.* 76/77, 67–76.
- O'Brien, S.R., Mayewski, P.A., Meeker, L.D., Meese, D.A., Twickler, M.S., Whitlow, S.I., 1995. Complexity of Holocene Climate as reconstructed from a Greenland ice core. *Science* 270, 1962–1964.
- Pachur, H.J., Wünnemann, B., Zhang, H., 1995. Lake evolution in the Tengger Desert, northwestern China, during the last 40,000 years. *Quat. Res.* 44, 171–180.
- Park, Y.A., Khim, B.K., Zhao, S., 1994. Sea level fluctuation in the Yellow Sea Basin (in Korean with English abstract). *J. Korean Soc. Oceanogr.* 29, 42–49.
- Pedersen, T.F., Calvert, S.E., 1990. Anoxia vs. productivity: what controls the formation of organic-carbon-rich sediments and sedimentary rocks? *AAPG Bull.* 74, 454–466.
- Pye, K., Zhou, L.P., 1989. Late Pleistocene and Holocene Aeolian dust deposition in north China and the northwest Pacific Ocean. *Palaeogeogr. Palaeoclimatol. Palaeoecol.* 73, 11–23.
- Qin, B.Q., Huang, Q., 1998. Evaluation of the climatic change impacts on the inland lake – a case study of lake Qinghai, China. *Clim. Change* 39, 695–714.
- Rea, D.K., 1994. The paleoclimatic record provided by eolian deposition in the deep sea: the geologic history of wind. *Rev. Geophys.* 32, 159–195.
- Rea, D.K., Leinen, M., 1988. Asian aridity and the zonal westerlies: Late Pleistocene and Holocene record of eolian deposition in the northwest Pacific Ocean. *Palaeogeogr. Palaeoclimatol. Palaeoecol.* 66, 1–8.
- Regnell, J., 1992. Preparing pollen concentrations for AMS dating – a methodological study from a hard-water lake in southern Sweden. *Boreas* 21, 373–377.
- Ren, G.Y., 1998. A finding of the influence of 'hard water' on radiocarbon dating for lake sediments in Inner Mongolia, China. *J. Lake Sci.* 10, 80–82.
- Ritchie, J.C., Haynes, C.V., 1987. Holocene vegetation zonation in the eastern Sahara. *Nature* 330, 645–647.
- Rhodes, T.E., Gasse, F., Ruifen, L., Fontes, J.Ch., Wei, K., Bertrand, P., Gibert, E., Mélières, F., Tucholka, P., Wang, Z., Chen, Z., 1996. A Late Pleistocene-Holocene lacustrine record from Lake Manas, Zhunggar (northern Xinjiang, western China). *Palaeogeogr. Palaeoclimatol. Palaeoecol.* 120, 105–121.
- Sarnthein, M., 1978. Sand deserts during glacial maximum and climatic optimum. *Nature* 272, 43–46.
- Shi, Y.F., Kong, Z.Z., Wang, S.M., Tang, L.Y., Wang, F.B., Yao, T.D., Zhao, X.T., Zhang, P.Y., Shi, S.H., 1993. Mid-Holocene climates and environments in China. *Glob. Planet. Change* 7, 219–233.
- Shi, Y.F., Kong, Z.Z., Wang, S.M., Tang, L.Y., Wang, F.B., Yao, T.D., Zhao, X.T., Zhang, P.Y., Shi, S.H., 1994. The climate fluctuation and important events of Holocene Megathermal in China. *Sci. China (Ser. B)* 37, 353–365.
- Shi, Y.F., Yao, T.D., Yang, B., 1999. Decadal climatic variations recorded in Guliya ice core and comparison with the historical documentary data from East China during the last 2000 years. *Sci. China (Ser. D)* 42, 91–100.
- Sirocko, F., Sarnthein, M., Erlenkeuser, H., Lange, H., Arnold, M., Duplessy, J.C., 1993. Century-scale events in monsoonal climate over the past 24,000 years. *Nature* 364, 322–324.
- Street-Perrott, F.A., Roberts, N., 1983. Fluctuations in closed-basin lakes as an indicator of past atmospheric circulation patterns. In: Street-Perrott, F.A., Beran, M.A., Ratcliffe, R.A.S. (Eds.), *Variations in the Global Water Budget*. Reidel, Hingham, MA, pp. 331–345.
- Stuiver, M., Reimer, P.J., Bard, E., Beck, J.W., Burr, G.S., Hughen, K.A., Kromer, B., McCormac, G., v.d. Plicht, J., Spurk, M., 1998. INTCAL98 Radiocarbon Age Calibration, 24,000–0 cal BP. *Radiocarbon* 40, 1041–1083.
- Sun, J.M., 2000. Origin of eolian sand mobilization during the past 2300 years in the Mu Su Desert. *China Quat. Res.* 53, 78–88.
- Sun, J.M., Ding, Z.L., Liu, T.S., 1998a. Desert distributions during the glacial maximum and climatic optimum: Example of China. *Episodes* 21, 28–31.

- Sun, J.M., Yin, G.M., Ding, Z.L., Liu, T.S., Chen, J., 1998b. Thermoluminescence chronology of sand profiles in the Mu Us Desert, China. *Palaeogeogr. Palaeoclimatol. Palaeoecol.* 144, 225–233.
- Sun, J.M., Ding, Z.L., Liu, T.S., Rokosh, D., Rutter, N., 1999. 580,000-year environmental reconstruction from Aeolian deposits at the Mu Us Desert margin, China. *Quat. Sci. Rev.* 18, 1351–1364.
- Sun, J.Z., Zhao, J.B., 1991. Quaternary of Loess Plateau in China. Science Press, Beijing.
- Ujiié, H., Ujiié, Y., 1999. Late Quaternary course changes of the Kuroshio Current in the Ryukyu Arc region, northwestern Pacific Ocean. *Mar. Micropaleontol.* 37, 23–40.
- Wang, H., Zhao, Q., Yu, L., Zhang, W., 1998. Late Quaternary eolian records in the northwest Pacific with Glacial cycles: a comparison. *Sci. China (Ser. D)* 41, 28–34.
- Wang, H.Y., Liu, H.Y., Cui, H.T., Abrahamsen, N., 2001. Terminal Pleistocene/Holocene paleoenvironmental changes revealed by mineral-magnetism measurements of lake sediments for Dali Nor area, southeastern Inner Mongolia Plateau, China. *Palaeogeogr. Palaeoclimatol. Palaeoecol.* 170, 115–132.
- Wang, L., Sarnthein, M., Erlenkeuser, H., Grimalt, J., Grootes, P., Heilig, S., Ivanova, E., Kienast, M., Pelejero, C., Pflaumann, U., 1999. East Asian monsoon climate during the Late Pleistocene: high-resolution sediment records from the South China Sea. *Mar. Geol.* 156, 245–284.
- Wang, S.M., Feng, M., 1992. The relationship between environmental change and strength of southeast monsoon in Daihai Lake, Inner Mongolia. *Sci. China (Ser. B)* 35, 722–734.
- Wei, K.Y., Yang, T.N., Huang, C.Y., 1997. Glacial-Holocene calcareous nannofossils and paleoceanography in the northern South China Sea. *Mar. Micropaleontol.* 32, 95–114.
- Wen, Q.Z., 1990. Geochemistry of Loess in China. Science Press, Beijing, in Chinese.
- Windom, H.L., 1975. Eolian contributions to marine sediments. *J. Sediment. Petrol.* 45, 520–529.
- Wünnemann, B., Pachur, H.J., 1998. Climatic and environment changes in the deserts of Inner Mongolia, China, since the Late Pleistocene. In: Alsharan, A.S., Glennie, K.W. and Whittle, G.L. (Eds.), *Quaternary Deserts and Climate Changes*. Balkema, Rotterdam, pp. 381–394.
- Yu, G., Prentice, I.C., Harrison, S.P., Sun, X.J., 1998. Pollen-based biome reconstructions for China at 0 and 6000 years. *J. Biogeogr.* 25, 1055–1069.
- Yu, G., Chen, X., Ni, J., Cheddadi, R., Guiot, J., Han, H., Harrison, S.P., Huang, C., Ke, M., Kong, Z., Li, W., Liew, P., Liu, G., Liu, J., Liu, Q., Liu, K.B., Prentice, I.C., Qui, W., Ren, G., Song, C., Sugita, S., Sun, X., Tang, L., Van Campo, E., Xia, Y., Xu, Q., Yan, S., Yang, X., Zhao, J., Zheng, Z., 2000. Palaeovegetation of China: a pollen database synthesis for the mid-Holocene and last glacial maximum. *J. Biogeogr.* 27, 635–664.
- Zhang, J., Lin, Z., 1992. *Climate of China*. Wiley, Shanghai.
- Zheng, X.Y., Zhang, M.G., Han, Z.M., Dong, Z.H., Zhang, B.Z., Gao, Z.H., Sun, D.P., Xue, C., Wang, K.J., 1992. *Salt Lakes in Inner Mongolia*. Science Press, Beijing, 195 pp., in Chinese.
- Zhou, W.J., Donahue, D.J., Porter, S.C., Jull, T.A., Li, X.Q., Stuiver, M., An, Z.S., Matsumoto, E., Dong, G.R., 1996. Variability of monsoon climate in East Asia at the end of the last Glaciation. *Quat. Res.* 46, 219–229.
- Zhou, W.J., Donahue, D.J., Jull, A.J.T., 1997. Radiocarbon AMS dating of pollen concentrated from eolian sediments: Implications for monsoon climate change since the Late Quaternary. *Radiocarbon* 39, 19–26.
- Zhou, W.J., Head, M.J., Lu, X.F., An, Z.S., Jull, A.J.T., Donahue, D., 1999. Teleconnection of climatic events between East Asia and polar, high latitude areas during the last deglaciation. *Palaeogeogr. Palaeoclimatol. Palaeoecol.* 152, 163–172.